21st Australian Fluid Mechanics Conference
Adelaide, Australia
10-13 December 2018

Low Reynolds number wakes of two Staggered Circular Cylinders

B. Liu and H. An

School of Engineering
The University of Western Australia, Perth, Western Australia, 6009, Australia

Abstract

Direct numerical simulations investigating the far-wake flow structures of two identical circular cylinders in the staggered arrangement at a Reynolds number of 150 is performed. Cylinder arrangements where L/D = 5, 10 and 20, and T/D = 0-5 are studied where L and T are the centre-to-centre longitudinal and transverse spacings respectively, and D is the cylinder diameter. Wake structures have been categorised into single and twin-wake regimes where the single-wake regime is observed to occur when T/D < 2 and twin-wake regime when T/D $\gtrsim$ 2. The single-wake regime features a secondary wake while the twin-wake regime features a locked-in wake for the majority of the T/D range studied. An analysis of the vortex shedding frequency and mean drag and lift coefficients with varying T/D is also provided.

Introduction

Fluid flow around cylindrical structures is a subject that has been investigated extensively due to its prevalence in various engineering structures. In reality, many engineering structures do not only consist of a single cylinder, but groups of multiple cylinders. Examples include offshore structures, chimneys, bridge piers, powerlines and heat exchangers. It is therefore, of great importance, that fluid flow around multiple cylinder groups is studied. Knowing the flow interactions between two cylinders provides the fundamental basis for understanding the behaviour of multiple cylinder groups, therefore, research on multiple cylinder arrangements to date has mainly focused on two-cylinder configurations. There are three general configurations that exist for two circular cylinders: tandem, side-by-side and staggered. These are categorised based on their relative orientation to the mean flow velocity U as shown in Figure 1. The geometry of two circular cylinders is described by the normalised centre-to-centre spacing between the cylinders where D is the diameter of the cylinder. These are defined as L/D in the longitudinal direction, applying to tandem cylinders, and T/D in the transverse direction, applying to side-by-side cylinders. For staggered cylinders, their geometry is defined using a combination of L/D and T/D, or instead, a centre-to-centre pitch P/D, and angle of incidence α.

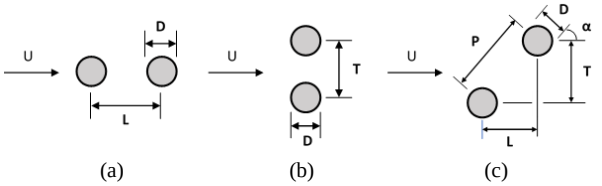

Figure 1. Arrangements of two identical circular cylinders: (a) Tandem; (b) Side-by-side; (c) Staggered

Zdravkovich [13] studied the flow interference between staggered cylinders within the range L/D = 0-5 and T/D = 0-5 at Re = 2.5×10^4 - 1.6×10^5 and identified three main types: wake interference, proximity interference and no interference. Wake interference was where the downstream cylinder (C2) was either completely, or at least partially, submerged in the wake of the upstream cylinder (C1), while proximity interference was where the wake of one cylinder affected that of the other, but neither was submerged in the wake of the other. It is to be noted that there have been some disputes with regards to the accuracy of the "no interference" region, which was observed at P/D $\gtrsim$ 3.75 and α $\gtrsim$ 35˚. The review paper by Sumner [8] stated that interference in the form of anti-phase vortex shedding synchronisation could be observed in the proposed "no interference" region. Sumner et al. [9] performed flow visualisation using Particle Image Velocimetry (PIV) for staggered cylinders arranged at P/D = 1-5 and α = 0-90˚, where Re = 850-1900. Sumner et al. [9] provided a detailed analysis and identified 9 different flow patterns that focused on the behaviour of the cylinders' shear layers, gap flow and vortex shedding interactions. The 9 flow patterns identified were categorised into three even groups, namely, single bluff body for closely spaced cylinders (P/D = 1-1.25), small incidence angle (P/D = 1.24-4, α = 0-30˚), and large incidence angle (P/D = 1.25-5, α = 15-90˚). Hu and Zhou [3] studied the near-wake flow structures for staggered cylinders arranged at P/D = 1.2-4 and α = 0-90˚, where PIV was used at Re = 7000 and Laser Induced Fluorescence (LIF) at Re = 300. Four flow modes were identified based on whether a single or twin vortex-street was observed and was further grouped by features such as wake structure, vortex strength and vortex-shedding frequency. Alam and Meyer [1] performed surface oil-flow visualisations at Re = 850-1900 for staggered cylinders at P/D = 1.1-6 and α = 0-180˚. Altogether 19 distinct flow categories were identified with particular attention being paid to the co-existence of multiple flow states, where one quadristable flow, three tristable flows, and four bistable flow modes were observed. Lee and Yang [6] presented four regime maps for Re = 40, 50, 100 and 160 in the range L/D = 0-6 and T/D = 0-6. Up to 10 flow patterns were identified in each flow map. The studies mentioned above have concentrated on understanding the flow behaviour of closely spaced cylinders arranged at configurations where L/D ≤ 6 and T/D ≤ 6. For L/D > 6, the effect of C2 on C1 diminishes rapidly with the increase of L/D, but the wake of C1 still has a considerable impact on C2 even for very large L/D values since the wake of C1 sustains for several hundred diameters. Relatively less research has been conducted for the wake of two staggered cylinders where L/D > 6. Cooper [2] studied the cylinder arrangements where L/D = 1.35-50 and T/D = 1-7.5 at Re = 10^4 - 1.25×10^5, however only looked at force coefficients and pressure distributions. Similarly, Price [7] studied cylinder arrangements where L/D = 6-18 and T/D = 0-2.42, but mainly focused on force data. Flow visualisation is important as it provides a means of explaining the flow modes that lead to the measured quantities observed. Without it, determining flow behaviour is prone to misinterpretation. Vakil [12] performed numerical simulations to visualise the flow, however this was limited to tandem cylinders arranged at L/D = 1.1-400 when Re = 1-40. No vortex shedding was observed in the investigated parameter range. As much research has been done on the flow patterns, flow interactions and near-wake flow structures for closely spaced staggered cylinders, this work aims to extend the current understanding by studying not only the flow features for larger L/D values but also the far-wake features. Cylinders spaced at L/D = 5-20, and T/D = 0-5 are studied using two-dimensional numerical simulations at Re = 150.

Governing equations

The continuity and incompressible Navier-Stokes equations are the governing equations of the flow and are given below:

$$\frac{\partial u_i}{\partial x_i} = 0 \quad (1)$$

$$\frac{\partial u_i}{\partial t} + u_j \frac{\partial u_i}{\partial u_j} = -\frac{1}{\rho}\frac{\partial p}{\partial x_i} + \nu \frac{\partial^2 u_i}{\partial x_i \partial x_j} \quad (2)$$

$(x_1, x_2) = (x, y)$ are Cartesian coordinates, u_i is the velocity component in the direction x_i, t is time and p is pressure. The equations are solved through Direct Numerical Simulations (DNS) using OpenFOAM (www.openfoam.org), an open source computational fluid dynamics (CFD) package. The model employed has been applied by [4] and [11] for simulating flow around circular cylinders at similar Reynolds numbers.

Numerical method

A rectangular computational domain is adopted. The upstream and downstream cylinders are located at 30D and 200D from the inlet and outlet boundaries respectively. The dimension of the domain in the crossflow direction is 100D, resulting in a blockage ratio of 0.01. The following boundary conditions are specified to the domain. A constant velocity (U, 0) is specified on the inlet boundary. At the outlet, the normal gradient of flow velocity is set to zero, and the pressure is specified as a reference value of zero. A 'symmetry' boundary condition is applied on the lateral boundaries. Due to the different geometrical arrangements involved with staggered cylinders, three main mesh types were necessary. One for the tandem configuration, one for arrangements with small T/D, and one for arrangements with larger T/D. These are shown in Figure 2. For the cases with small T/D, the mesh domain was created such that the mesh distribution was as uniform as possible by ensuring that the ratios of the divided mesh-regions were geometrically similar.

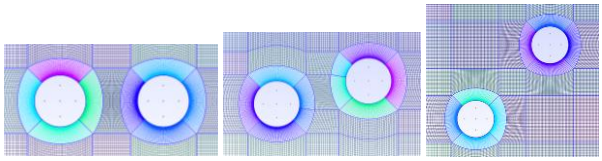

(a) (b) (c)

Figure 2. Typical meshes: (a) T = 0; (b) 0 < T/D < 1.27; (c) T/D ≥ 1.27

Single cylinder results

As a reference case, simulation results for the flow around a single cylinder are reported. Figure 3 shows the wake structure for this case. It shows that a Karman vortex-street with periodic vortex shedding is formed in the wake. The vortices gradually decay and are no longer identifiable when x/D > 70. Further downstream, a pair of parallel shear layers is formed. No secondary vortex-street is observed within 200D for this case which agrees well with [5] and [10]. The normalised vortex shedding frequency i.e. the Strouhal number is defined as $St = fD/U$, where f is the vortex shedding frequency. For a single cylinder, St = 0.184 and the mean drag coefficient C_D = 1.322. This is in good agreement with the existing literature.

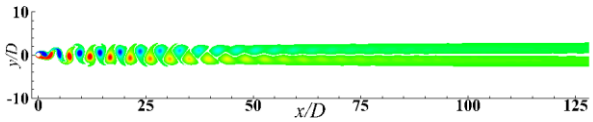

Figure 3. Wake structure for a single cylinder at Re = 150.

Wake structure of two cylinders

The wake structures for two cylinders arranged at L/D = 5, 10 and 20, and T/D = 0-5 are shown below in Figures 4-6.

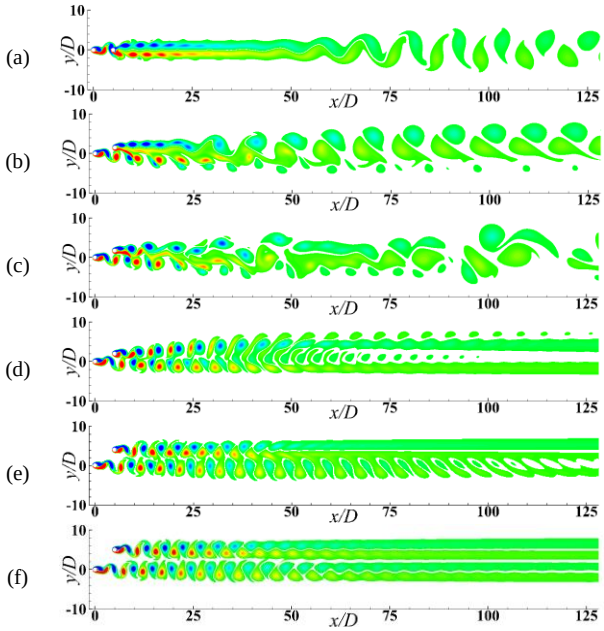

Figure 4. Wake structures when L/D = 5: (a) T/D = 0; (b) T/D = 1.5; (c) T/D = 1.75; (d) T/D = 2; (e) T/D = 4; (f) T/D = 5

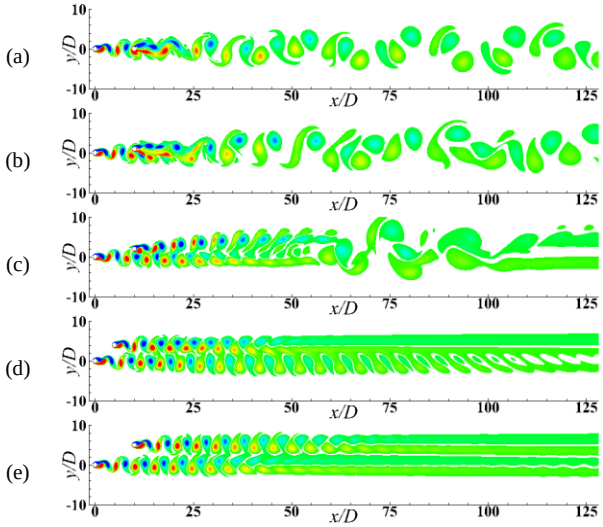

Figure 5. Wake structures when L/D = 10: (a) T/D = 0; (b) T/D = 1; (c) T/D = 2; (d) T/D = 4; (e) T/D = 5

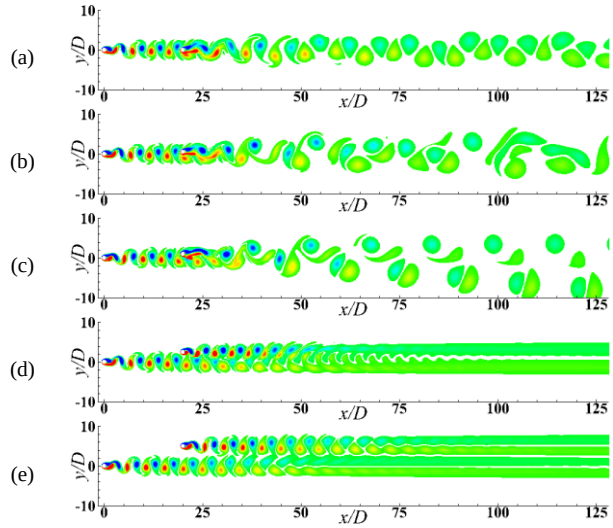

Figure 6. Wake structures when L/D = 20: (a) T/D = 0; (b) T/D = 0.5; (c) T/D = 1; (d) T/D = 2.5; (e) T/D = 5

In this work, wake structures are categorised based on whether a single or twin wake is observed. For L/D = 5, 10 and 20, a single-wake is observed when T/D < 2. These also feature a secondary wake (SW) that is formed closer to C2 as either L/D or T/D is increased. For example, in Figure 4a (L/D = 5 and T/D = 0), the SW is formed after all the vortices in the primary wake have fully decayed. However, as T/D is increased to 1.5, the SW is formed directly by the merging of vortices in the primary wake (Figure 4b, x/D > 25). For T/D = 1.75 (Figure 4c), the SW becomes irregular. As T/D is further increased to T/D $\gtrsim$ 2 (Figure 4d ~ f), a twin-wake emerges where two rows of vortices are observed at least in the near-wake. For cases in the in the single-wake regime, the interactions between the vortices generated from the two cylinders are very strong such that a SW is formed (Figure 4a ~ c). With increasing T/D however, the interactions between the wakes of the two cylinders are alleviated so as to not cause the formation of a SW, but rather wake synchronisation (or lock-in) (Figure 4d ~ f). These observations agree with [8] who disputed the "no interference" region proposed by [13] and also observed synchronisation of the two wakes in this region. Only when T/D $\approx$ 5, are the wakes of C1 and C2 no longer synchronised, but have minimal interaction.

Vortex shedding frequency

The vortex shedding frequency is analysed based on the spectra for lift coefficient C_L. For L/D = 5 (Figure 7), the two cylinders have the exact same vortex shedding frequency for all the T/D values investigated. In Figure 7a, besides the dominating vortex shedding frequency (St_1 = 0.160), a higher harmonic frequency $3St_1$ also exists in the spectrum. When T/D is increased to 1 (Figure 7b), a strong peak appears at $2St_1$. This is because the flow (especially for that behind C2) loses its temporal-spatial symmetry with respect to the streamwise centreline of C2. This can be explained by conducting Dynamic Mode Decomposition on the flow field. No detail is given here due to the page limit. With further increase of T/D, the energy level of $2St_1$ decreases gradually and almost vanishes at T/D = 5 (Figure 7d). This is because the wake of C2 regains its temporal-spatial symmetry.

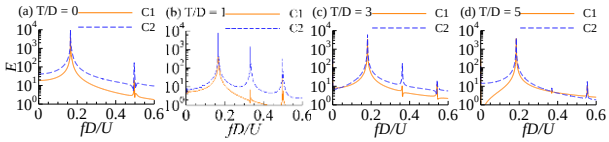

Figure 7. Power spectra densities for L/D = 5.

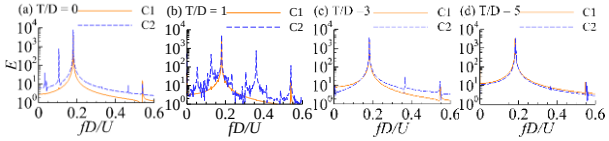

Figure 8. Power spectra densities for L/D = 10.

The spectra for L/D = 10 are given in Figure 8. When the two cylinders are arranged in tandem (Figure 8a), the dominating frequency for the two cylinders is the same, but two strong lower frequency components appear in the spectrum of C2 with fD/U = 0.106 and 0.032. Here fD/U = 0.106 represents the vortex shedding frequency in the SW formed after C2 (Figure 5a) and fD/U = 0.032 represents the waviness of the SW. When T/D is increased to 1, the SW behind C2 becomes irregular (Figure 5b), which explains the rough spectrum of C2 in (Figure 8b). Two lower frequency peaks can also be identified here, meanwhile $2St_1$ also appears in the spectrum for C2. For T/D = 3 and 5 (Figure 8c and d), the low frequency components disappear due to wake lock-in. Similar features can be found for L/D = 20, so no further details about their frequency spectra are given here.

Figure 9 presents the St numbers for both C1 and C2 based on the spectra for C_L and have been normalised by the single cylinder value. Most cases show that both cylinders have an identical dominant St number. This is due to either wake lock-in or the upstream shed vortices dominating vortex shedding in C2. At T/D = 5 for L/D = 10 and 20 however, C2 is observed not only to have a different St number to C1, but also a slightly higher value than the single cylinder value. This is because there is no wake lock-in and the mean flow velocity in the region of C2 is slightly higher than the freestream velocity. Although the wake structures observed in Figure 5 (d) and (e) are very similar, the fundamental difference between the two cases is that vortex shedding for C1 and C2 is locked-in at T/D = 4 but not at T/D = 5 as shown in Figure 9b. This is further illustrated by plotting the lift force time histories of C1 and C2 against each other in Figure 10. The duration of the lift force time histories is 120 vortex shedding periods from C1. The diagram in Figure 10a is a single loop, which indicates synchronised vortex shedding behaviour. In contrast, Figure 10b covers a large area, which is due to the different vortex shedding frequencies of the two cylinders when T/D = 5. This comparison demonstrates that there is a critical T/D value between 4 and 5, beyond which the vortex shedding process of the two cylinders are no longer locked-in. For smaller L/D, St is observed to be more sensitive to changes in geometry.

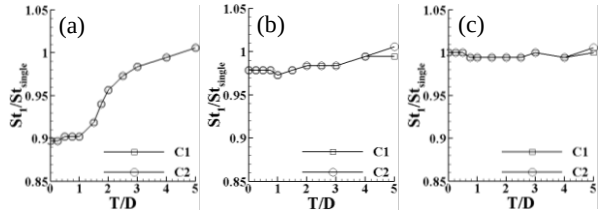

Figure 9. Strouhal number graphs normalised by the single cylinder value: (a) L/D = 5; (b) L/D = 10; (c) L/D = 20.

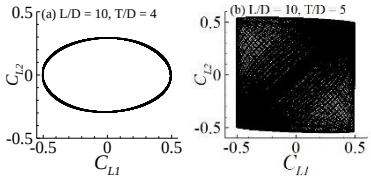

Figure 10. Lift force diagram for the two cylinders with locked-in (a) and no lock-in (b) vortex shedding features.

Secondary wake frequencies

Figure 11 shows the SW frequency (St_2) and its relationship with the dominant frequency (St_1). For L/D = 5, St_2 is obtained by analysing the vertical velocity time history in the far-wake since the SW is too far away to be detected by the lift force time history of C2. In general, it is observed that for low T/D, the relationship between St_1 and St_2 is relatively steady. However, with increasing T/D, there comes a point where St_2 increases rapidly and approaches the value of $0.8St_1$. This abrupt change becomes less evident as L/D is increased. It is also observed that for low T/D, the ratio between St_2 and St_1 for L/D = 5 is 0.5, while for L/D = 10 and 20, the ratio is approximately 0.6. This is due to the immediate formation of the SW behind C2 such that not all vortices are able to merge.

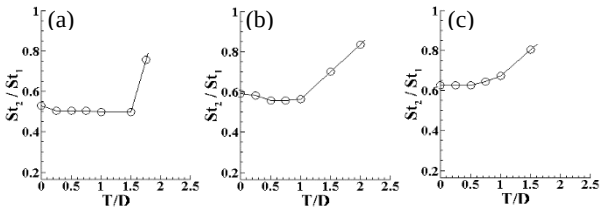

Figure 11. Secondary wake frequency for C2 where St_2 is normalised by St_1: (a) L/D = 5; (b) L/D = 10; (c) L/D = 20

Forces

Mean Lift coefficient

Figure 12 shows the mean lift coefficients for the cylinder arrangements studied. The mean lift of C1 is observed to be relatively close to 0 since the vortices shed from the top and bottom sides have similar strength. For C2, as T/D is increased, the mean lift features a negative lift peak at $0 < T/D \lesssim 2$. The negative lift force acting on C2 is due to the wake of C1 inducing a relatively lower pressure on the lower side of C2. It is observed that the negative lift peak for L/D = 10 is significantly smaller than those observed when L/D = 5 and 20.

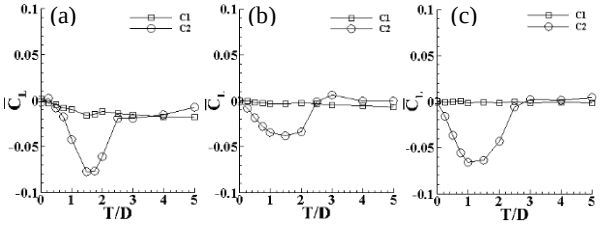

Figure 12. Mean lift coefficient graphs: (a) L/D = 5; (b) L/D = 10; (c) L/D = 20

Mean Drag coefficient

Figure 13 presents the mean drag coefficients for the cylinder arrangements studied. The mean drag of C1 is observed to be relatively constant, however for smaller L/D, a slight increasing trend can be observed as T/D is increased. For C2, the mean drag starts off significantly lower than C1 since the presence of C1 in front of C2 shelters the oncoming flow onto C2. As T/D is increased, the mean drag also increases such that the mean drag on C2 is slightly higher than C1. This occurs since the drag forces experienced by C2 is mainly dominated by the mean flow velocity in the wake of C1, where above a certain T/D value, the mean flow velocity surpasses that of the freestream velocity. Vortex-vortex interactions between the two cylinders are also observed to slightly increase drag, agreeing with [1].

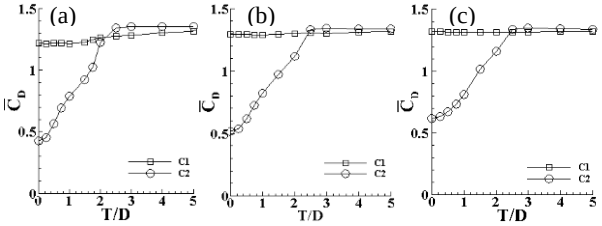

Figure 13. Mean drag coefficient graphs: (a) L/D = 5; (b) L/D = 10; (c) L/D = 20

Conclusion

Two-dimensional numerical simulations were conducted at Re = 150 to investigate the far-wake features of two circular cylinders where L/D = 5, 10 and 20, and T/D = 0-5. The conclusions are summarised as follows:

- A single wake featuring a secondary wake was observed when T/D < 2, while a twin wake was observed when $T/D \gtrsim 2$. The majority of the twin wake regime featured a locked-in wake between C1 and C2 as reflected by the matching St numbers between the two cylinders.
- Only when $T/D \approx 5$ were the St numbers from C1 and C2 different, where the St number for C2 was higher than the single cylinder value due to a greater mean flow velocity.
- St_2 was observed to be half that of St_1 for low T/D when L/D = 5 since the secondary wake was far enough to allow consistent merging between vortices. When L/D = 10 and 20 however, $St_2 \approx 0.6St_1$ due to the immediate formation of the secondary wake behind C2 preventing some vortices to merge.
- Larger T/D values resulted in the approach of wake lock-in where St_2 quickly approached that of St_1 such that a secondary wake was no longer observed.
- A negative mean lift on C2 was found in the range of $0 < T/D \lesssim 2$. As for mean drag, the forces experienced by C2 were mainly dominated by the mean flow velocity in the wake of C1, where the drag on C2 was initially very small, then rose with increasing T/D such that it surpassed that of C1.

Acknowledgements

This work was supported by resources provided by the Pawsey Supercomputing Centre with funding from the Australian Government and the Government of Western Australia.

References

[1] Alam, M.M. & Meyer, J.P., Two interacting cylinders in cross flow, *Physical Review E*, **84**, 2011, 056304.

[2] Cooper, K.R., Wind tunnel measurements of the steady aerodynamic forces on a smooth circular cylinder immersed in the wake of an identical cylinder, *National Research Council of Canada*, 1974, LTR-LA-119.

[3] Hu, J. & Zhou, Y., Flow structure behind two staggered circular cylinders. Part 1. Downstream evolution and classification. *Journal of Fluid Mechanics*, **607**, 2008, 51-80.

[4] Jiang, H., Cheng, L., Tong, F., Draper, S. & An, H., Stable state of Mode A for flow past a circular cylinder. *Physics of Fluids*, **28**, 2016, 104103.

[5] Kumar, B. & Mittal, S., On the origin of the secondary vortex street. *Journal of Fluid Mechanics*, **711**, 2012, 641-666.

[6] Lee, K. & Yang, K.-S., Flow patterns past two circular cylinders in proximity. *Computers & Fluids*, **38**, 2009, 778-788.

[7] Price, S., The origin and nature of the lift force on the leeward of two bluff bodies. *The Aeronautical Quarterly*, **27**, 1976, 154-168.

[8] Sumner, D., Two circular cylinders in cross-flow: A review. *Journal of Fluids and Structures*, **26**, 2010, 849-899.

[9] Sumner, D., Price, S. & Paidoussis, M., Flow-pattern identification for two staggered circular cylinders in cross-flow. *Journal of Fluid Mechanics*, **411**, 2000, 263-303.

[10] Thompson, M. C., Radi, A., Rao, A., Sheridan, J. & Hourigan, K., Low-Reynolds-number wakes of elliptical cylinders: from the circular cylinder to the normal flat plate. *Journal of Fluid Mechanics*, **751**, 2014, 570-600.

[11] Tong, F., Cheng, L., Zhao, M. & An, H., Oscillatory flow regimes around flow cylinders in a square arrangement under small KC and Re conditions. *Journal of Fluid Mechanics*, **769**, 2015, 298-336.

[12] Vakil, A & Green, S., Numerical Study of Two-Dimensional Circular Cylinders in Tandem at Moderate Reynolds Numbers. *Journal of Fluids Engineering*, **135**, 2013, 071204.

[13] Zdravkovich, M.M., The effects of interference between circular cylinders in cross flow, *Journal of Fluids and Structures*, **1**, 1987, 239-261.